Simultaneous EEG-fMRI Acquisition at Low, High and Ultra-High Magnetic Fields up to 9.4T: Perspectives and...

Article *in* NeuroImage · June 2013

DOI: 10.1016/j.neuroimage.2013.06.048 · Source: PubMed

4 authors, including:

Irene Neuner
Forschungszentrum Jülich
67 PUBLICATIONS **932** CITATIONS
SEE PROFILE

Jorge Arrubla
Profil
26 PUBLICATIONS **142** CITATIONS
SEE PROFILE

N. Jon Shah
Forschungszentrum Jülich
573 PUBLICATIONS **13,965** CITATIONS
SEE PROFILE

NeuroImage 102 (2014) 71–79

Contents lists available at ScienceDirect

NeuroImage

journal homepage: www.elsevier.com/locate/ynimg

Review

Simultaneous EEG–fMRI acquisition at low, high and ultra-high magnetic fields up to 9.4 T: Perspectives and challenges

Irene Neuner [a,b,d,*], Jorge Arrubla [a], Jörg Felder [a], N. Jon Shah [a,c,d]

[a] Institute of Neuroscience and Medicine 4, INM 4, Forschungszentrum Jülich, Germany
[b] Department of Psychiatry, Psychotherapy and Psychosomatics, RWTH Aachen University, Germany
[c] Department of Neurology, RWTH Aachen University, Germany
[d] JARA – BRAIN – Translational Medicine, Germany

ARTICLE INFO

Article history:
Accepted 13 June 2013
Available online 22 June 2013

Keywords:
Low magnetic field
Ultra-high magnetic field
MR
EEG
Cardiac-related artefact

ABSTRACT

In this perspectives article we highlight the advantages of simultaneous acquisition of electroencephalography (EEG) and functional magnetic resonance imaging (fMRI). As MRI moves towards using ultra-high magnetic fields in the quest for increased signal-to-noise, the question arises whether combined EEG–fMRI measurements are feasible at magnetic fields of 7 T and higher. We describe the challenges of MRI–EEG at 1.5, 3, 7 and 9.4 T and review the proposed solutions. In an outlook, we discuss further developments such as simultaneous trimodal imaging using MR, positron emission tomography (PET) and EEG under the same physiological conditions in the same subject.

Contents

Introduction

The two cardinal tasks of imaging in neuroscience are the assessment of structure and function. Magnetic resonance imaging (MRI) is a non-invasive imaging technique that can be used to study a wide range of ages from new born child to the elderly. Longitudinal studies can be performed to monitor structural changes in the brain due to healthy neurodevelopment and ageing or due to interventions such as training, medication or neurosurgery. Voxel-based morphometry and diffusion tensor imaging (DTI) (Basser et al., 1994) with high spatial resolution provide a detailed look into the structure of the brain for the investigation of a wide range of diseases, such as epilepsy (Braakman et al., 2012), Alzheimer's disease (Kilimann et al., in press; Yang et al., 2012), Parkinson's disease (Cochrane and Ebmeier, 2013), Tourette syndrome

* Corresponding author at: Institute for Neuroscience and Medicine 4, INM4, Forschungszentrum Jülich, 52425 Jülich, Germany. Fax: +49 2461 611919.
E-mail address: i.neuner@fz-juelich.de (I. Neuner).

1053-8119/$ – see front matter © 2013 Elsevier Inc. All rights reserved.
http://dx.doi.org/10.1016/j.neuroimage.2013.06.048

(Neuner et al., 2010a), bipolar disorder (Selvaraj et al., 2012) and schizophrenia (Kuswanto et al., 2012). For studying functional aspects of the brain, functional magnetic resonance imaging (fMRI) has successfully been applied in the assessment of myriad cognitive, emotional and social tasks (Cabeza and Nyberg, 2000; Huettel, 2012; Neuner et al., 2007, 2010b; Ochsner et al., 2012; Rushworth et al., 2013; Shah et al., 2001). However, the main drawback of fMRI is its dependence on the blood oxygenation level dependent (BOLD) effect (Ogawa et al., 1993). The BOLD effect is the signal change observed due to the change in blood oxygenation in response to localised neuronal activity. The timescale of the BOLD response is on the order of seconds after the neuronal activity, which results in a low functional temporal resolution.

Electroencephalography (EEG) assesses neuronal function on a millisecond time scale (Makeig et al., 2004; Michel and Murray, 2012). Despite the fact that EEG is a well established and routinely used tool for diagnostic and research purposes, there is currently no clear understanding of how the measured scalp EEG signals represent the spatiotemporal organization of the underlying neuronal activity. It has long been proposed that scalp EEG signals depend on a) the amplitudes and b) on the spatial synchronization of underlying neural activity. In simultaneous intracranial and surface EEG experiments in monkeys, Musall et al. investigated this question (Musall et al., in press). They reported that trial-by-trial fluctuations in EEG power are the result of a linear combination of local field potentials (LFPs) and interelectrode temporal synchrony. Musall and coworkers gave particular emphasis to the fact that a potential dissociation between EEG and fMRI signals could be due to neural synchrony (Buzsáki and Draguhn, 2004; Meltzer et al., 2009; Musall et al., in press; Nunez and Silberstein, 2000; Yeşilyurt et al., 2010). They discuss that synchronization among a large population of neurons could be less metabolically demanding and therefore could explain an increase in the EEG signal accompanied by a decrease in BOLD signal (Musall et al., in press).

Recently, the simultaneous acquisition of fMRI and EEG data has been developed to synergistically combine their good spatial and temporal resolutions, respectively (Huster et al., 2012; Laufs et al., 2008; Neuner et al., 2010b). The development of simultaneous fMRI and EEG was initially driven by clinical needs in pharmaco-resistant epilepsy patients undergoing pre-neurosurgical assessment (Ives et al., 1993; Thornton et al., 2010a, 2010b; Vulliemoz et al., 2011). Simultaneous fMRI and EEG permits the investigation of a scientific or clinical question in one individual at the same time under exactly the same physiological and technical conditions. It is particularly desirable in experimental designs when a parallel paradigm might evoke confounding effects, for example in pharmacological challenges or in paradigms relying on novelty effects. The simultaneous approach is also important for the investigation of resting state functional connectivity (Biswal et al., 1995; Laufs, 2012; Raichle et al., 2001) and can help to distinguish a "resting state" from an early sleep state (Tagliazucchi et al., 2012). It also allows for the analysis of oscillation amplitude fluctuations; a neuronal activity phenomenon which reflects functional states and can be used in the definition of different states e.g. in sleep research. These fluctuations in oscillation amplitude have been demonstrated to affect behaviour when occurring in context with a task (Makeig et al., 2004).

Functional MRI and EEG data are complementary in terms of spatial and temporal resolution, however, the simultaneous acquisition of fMRI and EEG data comes not without associated complications. Recording EEG during fMRI measurements requires an MR-compatible EEG-system, which are now commercially available. Care must be taken however to ensure the safety and comfort of the subjects and to provide good data quality (Debener and Herrmann, 2008; Neuner et al., 2010b). EEG data acquired during simultaneous MRI acquisition suffer from two types of artefact: the so-called cardiac-related or pulse artefact and the gradient artefact caused by magnetic field gradients switching during any applied MR-sequence. Their origin will be discussed in more detail in the second part of the review. Both artefacts can be successfully removed from the EEG data by different methods, such as Average Artefact Subtraction (AAS) (Allen et al., 2000) Optimal Basis Set (OBS) (Niazy et al., 2005) or Independent Component Analysis (Eichele et al., 2009; Jung et al., 2000).

Simultaneously acquired EEG–fMRI data are a prerequisite for single trial experiments. In a classical monomodal or sequential approach the trial-to-trial evoked response variability is averaged out. However, these data could broaden our understanding of functional neuronal networks. In single trial experiments, e.g. prepulse pulse inhibition (PPI) of the startle reflex or of P300 latencies and amplitudes, Electromyography- or EEG-informed fMRI analysis becomes feasible (Bagshaw and Warbrick, 2007; Debener et al., 2006, 2007; Neuner et al., 2010b). The combination of EEG and fMRI allows one to investigate the fluctuations in evoked responses as well as spontaneous activity changes, e.g. during "resting state". Such fluctuations are believed to mirror variability in human perception and behaviour (Sadaghiani et al., 2010a, 2010b).

As MRI moves towards ever higher magnetic field strength in the quest for increased sensitivity to the BOLD effect (as well as other motivations), the question arises whether the simultaneous approach would still be feasible. A major challenge to meet is the fact that the cardiac-related artefact is known to increase linearly with the magnitude of the B0 field, and therefore the problem of artefact correction should be revisited. Here we review the status quo of simultaneous fMRI–EEG experiments at low, high and ultra-high magnetic fields with regard to acquisition and analysis challenges.

EEG–fMRI Acquisition at 1.5 T and 3 T

Artefacts

A significant disadvantage of measuring EEG at magnetic fields is the contamination of the signal as consequence of the MR scanner environment and sequences. The artefacts which affect the EEG signal are discussed below.

Gradient artefact

The "gradient artefact" is caused by the switching of the magnetic field gradients used for spatial encoding during fMRI data acquisition. The changing magnetic fields induce a potential difference in the EEG leads that appears in the measurement as large oscillations. The timing of this switching is inherent to the MR sequence and is well characterised. Therefore, correction of the gradient artefact by e.g. Average Artefact Subtraction (Allen et al., 1998) or modifications thereof (e.g. Moosmann et al., 2009) works well. For EEG-data monitoring during acquisition at 1.5 T and 3 T, online correction software is commercially available.

Pulse artefact

The "pulse artefact" or "cardiac-related artefact" is caused by the cardiac cycle. A recent technical note by Mullinger et al. (Mullinger et al., 2013) investigated, in a very systematic way, potential sources of the pulse artefact. Three main mechanisms contribute to the generation of the artefact (Allen et al., 1998; Bonmassar et al., 2002; Debener et al., 2008; Huang-Hellinger et al., 1995; Mullinger et al., 2013; Müri et al., 1998; Tenforde et al., 1983; Yan et al., 2010):

a) During the cardiac cycle the head rotates slightly (driven by alterations in the momentum of the pulsatile blood flow in the cranial arteries). This head movement causes the EEG leads to move through the magnetic field of the MR scanner which induces a voltage over the EEG leads.
b) Since blood is an electrically conducting fluid flowing within a magnetic field the Hall effect results in a separation of charge which, in turn, leads to a variation of the voltage at the scalp surface.
c) Driven by pulsatile blood flow, the scalp expands and causes movement of the EEG leads through the magnetic field.

Correction of the cardiac-related artefact poses a greater challenge due to its variability over cardiac cycles and different electrodes positions. In addition, the cardiac-related artefact shows a marked variability with B0 strength. This will be discussed in more depth later in the text.

Compressor artefact

It is a well established fact, that the helium compressor at the MR scanner is a source of artefacts in the EEG signal (Nierhaus et al., 2013; Ritter et al., 2010), which induces vibration in the cryopump system. The helium pump induces artefacts in the frequency spectrum of the EEG with additional broad band frequency power starting usually at 20–30 Hz (Nierhaus et al., 2013). The contribution to noise from the compressor seems to be variable and highly dependent of the mounting of the cold heads. For example, the cold heads of the prototype 9.4 T Siemens (Siemens, Erlangen, Germany) scanner in the Research Centre Jülich (Germany) are mounted on extended turrets in order to operate in a lower magnetic field environment; as a result it has no significant contribution to the noise levels in the EEG recording (Fig. 1). In contrast, a commercial 3 T TRIO Siemens scanner in the same institute has its cold heads mounted directly on the 3 T magnet vessel, resulting in contamination of the EEG signal.

Set up

For recording simultaneous EEG–fMRI data a few pragmatic points should be considered in order to improve data quality. This relates to system set up, volunteer/patient positioning, data acquisition and data modelling. Whatever methods one chooses to minimize the cardiac-related artefact and independent of the method of choice for correction, the basic principle "the better your raw data quality is, the better your post-processed data can be" is valid at any given field strength (Fig. 2).

With regard to the set-up, the use of a synchronization device between MR scanner clock and EEG recording software is essential in order to apply Average Artefact Template Subtraction (Allen et al., 1998) for the correction of the gradient artefact in the most accurate way and for synchronization of stimulus onset and EEG–fMRI data. In order to improve the cardiac-related artefact correction a better raw signal could be obtained by recording the electrocardiogram (ECG) via chest electrodes (Fig. 3) with an additional bipolar MR-compatible amplifier (Leclercq et al., 2009). Another, but experimental custom-made approach for an improved correction is the use of an optical motion tracking system (Levan et al., 2013). Positioning of the subject and the EEG system in the MR scanner is also a matter of interest. In order to prevent heating of the EEG cables, they should be routed properly with respect to the electrical fields produced by the RF coil. Small variations of the cable position might, in the worst case, create significant heating; for that purpose the cables should be kept in position and overlaid with sand bags. In order to record high quality data, the amplifier(s) should be protected from vibrations of the inner scanner housing either by sand bags put below the amplifiers or by setting up the amplifiers outside the end of the MR scanner on a separate MR-compatible table.

With regard to volunteer/patient set up the following steps could help in minimizing the artefacts. Mullinger et al. describe the reduction of the cardiac-related artefact by using an evacuated head cushion, a bite bar individually adapted to each subject and a swimming silicon cap as an isolating sheet between the scalp and the electrodes (Mullinger et al., 2013).

Before starting data acquisition in a simultaneous EEG–fMRI measurement the planned MR sequences have to be evaluated with regard to SAR deposition. Several groups acquire structural anatomical MR data before acquiring functional data with the EEG equipment in place. A recent paper by Nöth et al. (2012) emphasized that only MR sequences with low specific absorption rate (SAR) level should be used. Sequences such as T1-weighted sequences (FLASH, MPRAGE, MDEFT) with SAR below the values for functional MRI sequences based on gradient EPI are reported to be safe (Nöth et al., 2012).

With regard to analysis, Chaudhary et al. showed the importance of modelling confounding events such as eye blinks or swallowing in order to improve data sensitivity and quality in search for epileptic activity in patients (Chaudhary et al., 2012).

Perspectives

EEG data reported in the literature from simultaneous EEG–fMRI measurements are usually surface EEG data. Carmichael et al. were the first to report intracranially acquired EEG data in epilepsy patients during fMRI at 1.5 T (Carmichael et al., 2012). Intracranial electrodes could also contribute to the further investigation of the relationship between electrophysiological signals and the BOLD-effect as well as to research in neurovascular coupling in general (Singh, 2012). Other experimental approaches which aim at establishing a trimodality e.g. MR–PET–EEG (Neuner et al., 2013b) and simultaneous transcranial magnetic stimulation (TMS)-MR–EEG (Peters et al., 2013) open the possibility for selective stimulation or inhibition of a given target area to study its effect and changes in connectivity patterns.

EEG–FMRI at ultra-high fields

Status quo and perspectives

In the previous part of this review the advantages and disadvantages of combining EEG and fMRI were explored and it was demonstrated that such multimodal measurements represent an attractive tool for the investigation of human brain function *in vivo*. The focus of this section is to portray the emerging implementation of simultaneous EEG in ultra-high magnetic fields.

One key characteristic of MRI is its tunable soft tissue contrast based on, for example, T1 and T2 relaxation times, proton density, and diffusion/flow properties. Ultra-high fields, defined as ≥7 T, facilitate structural imaging with significantly higher spatial resolution, higher functional (BOLD) contrast (Olman et al., 2012) as well as different BOLD contrasts (Yacoub et al., 2005). In addition, achieving sub-millimetre resolution in human subjects during fMRI experiments is essential to permit layer-specific activation profiles to be detected (Olman et al., 2012). With improved signal-to-noise-ratio (SNR) at ultra-high magnetic fields, not only the signal changes appear to be most robust, but also the reliability and reproducibility of the fMRI experiments increase (Harel et al., 2006). Given their complementary properties, the simultaneous recording of EEG and fMRI at ultra-high magnetic fields is desirable for cognitive neuroscience, in particular, studies investigating neuro-vascular coupling, pharmacological challenge studies, resting state studies, sleep studies, studies investigating epilepsy or evoked potential studies (Caballero-Gaudes et al., 2013; Debener and Herrmann, 2008; Juckel et al., 2012; Koike et al., 2011; Rosenkranz and Lemieux, 2010). As it was mentioned in the EEG–fMRI acquisition at 1.5T and 3T section, important considerations towards the safety and well being of participating subjects are mandatory, and this is particularly important at ultra-high fields. Common effects of the ultra-high magnetic fields on human subjects are dizziness, nystagmus, phosphenes (light flashes), and head ringing (Heinrich et al., 2013). Such effects appear predominantly while the subject is being moved inside the scanner bore and commonly disappear in a few minutes after the subject reaches the isocentre. Severe effects are rare and include nausea, vertigo and vomiting. Another important safety concern arises from the higher RF power required to generate a given B1-field strength. A reduction in RF wavelength may lead to greater interaction of the applied RF with the electrodes and wires of the EEG system (Lemieux et al., 1997).

As MRI moves towards ultra-high field imaging the question of whether simultaneous EEG recording would still be feasible needs to be

addressed. EEG data acquired at 7 T (Debener et al., 2008; Mullinger et al., 2008b) and 9.4 T (Neuner et al., 2013a) show that the cardiac-related artefact increases substantially (Fig. 4) and is more challenging to remove from the data, but that in principle EEG and event-related potential (ERP) data recording is feasible (Neuner et al., 2013a). Debener et al. found that the amplitude of the cardiac-related artefact scaled linearly with the static magnetic field strength (Debener et al., 2008), which was in line with theoretical assumptions of the Lorentz' law (Tenforde et al., 1983). In the study conducted by Neuner and co-workers this assertion was further confirmed with data recorded at a static magnetic field of 9.4 T (Neuner et al., 2013a). See Fig. 4.

One of the first EEG recordings performed at ultra-high magnetic field of 7 T took place in 2000 by Van Audekerkea et al. (2000). On that occasion a special RF-antenna was designed for simultaneous MRI and EEG acquisition at 7 T. It was later in 2006 when the group of Vasios and co-workers performed the first combined EEG–fMRI experiment using a new EEG cap named "Ink Cap" (Vasios et al., 2006), resulting in low distortion of the functional images and also good EEG quality. The feasibility of recording simultaneous EEG–fMRI at 7 T was further explored in a study conducted by Mullinger et al. (2008a). On that occasion no significant safety concerns were identified on phantom or human experiments and EEG data allowed for identification of alpha-band related desynchronisation related to visual stimulation. A standard EPI sequence was used for acquisition of functional data, where no significant heating was found (less than 0.4 °C) during the measurements. Analysis of the functional data showed sensible results according to the visual stimulation. During this experiment the helium pump was turned off since the team found significant noise contribution from the compressor to the EEG data. Later in 2009 Brookes and co-workers successfully applied source localisation via the beamformer algorithm from EEG recorded at 3 T to 7 T (Brookes et al., 2008, 2009). It was also demonstrated that EEG data in the gamma-band could be recorded successfully from human subjects at 7 T.

The electrodes in the EEG cap are a potential source of magnetic field inhomogeneity. The effect of EEG cap is a small reduction in the SNR, proportional to the number of electrodes. This arises probably from decreased B0 homogeneity due to residual magnetic susceptibility of the electrodes. Good shielding of the EEG electronics should

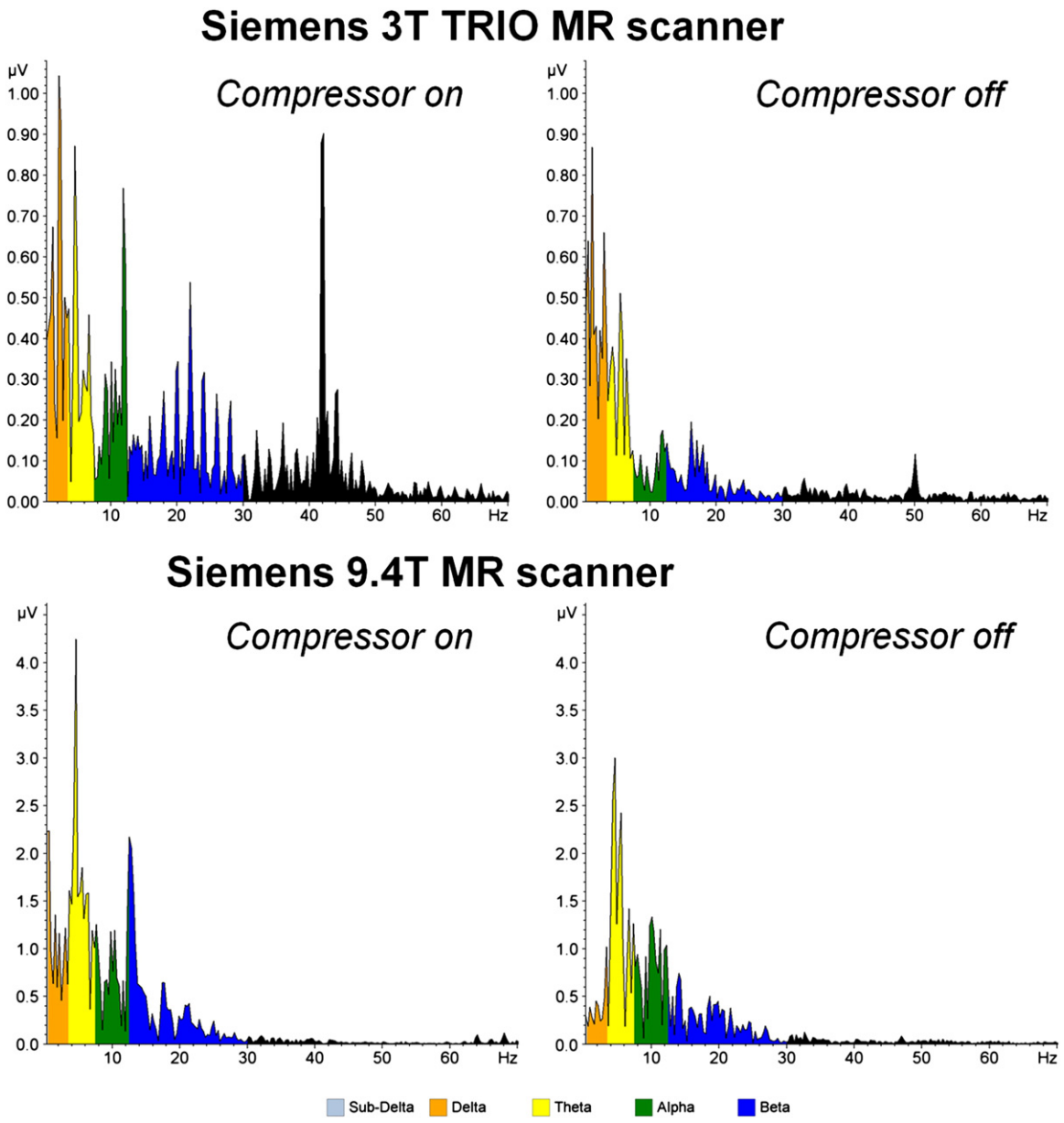

Fig. 1. Fast Fourier transform analysis of EEG resting state data, recorded in a Siemens 3 T Trio MR scanner and a Siemens 9.4 T MR scanner with the helium compressor turned on and turned off.

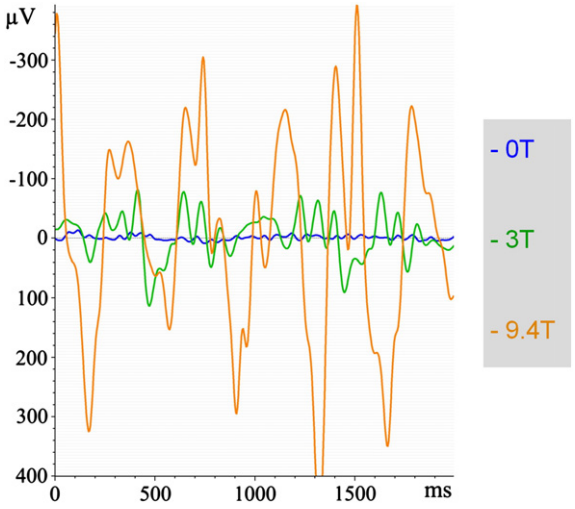

Fig. 2. Two-second epochs of raw EEG signal recorded at different magnetic fields: 0 T, 3 T and 9.4 T.

help in reducing the effect of electronic noise introduced into the MR receive coil. Even though the dense-array EEG systems (>64 channel) reduce the anatomic signal in some brain areas during fMRI measurements, the image signal-to-noise ratio and the extent of the BOLD signal is comparable with and without the EEG cap (Luo and Glover, 2012). From the experiments performed at 7 T, the SNR of fMRI recordings at such magnetic field with EEG are still superior to those recorded at 3 T without EEG (Mullinger et al., 2008b).

Recently it was demonstrated that from a technical point of view the electrophysiological recordings at ultra-high magnetic field of 9.4 T are possible (Neuner et al., 2013a). The results of the study of Neuner and co-workers showed that from the data-quality point of view, the cardiac-related artefact at 9.4 T could not be sufficiently reduced by standard methods such as OBS and AAS and this led to sub-optimal correction. Although there was an evident difficulty in correcting the data for the cardiac-related artefact, it was possible to identify auditory evoked potentials (Fig. 5) and event related spectral perturbations around the alpha-band in a large percentage of the subjects (Fig. 6). These results were only achieved when ICA was used to identify the components that contributed either to the ERP signal or to the alpha-band signal. The alpha-desynchronisation was identifiable even though there was contamination from a wide range of frequencies with increased power that were possibly linked to the effect of the static magnetic field on the EEG signal. From those results it was also possible to infer that the speed of sensory perception was not altered by the static 9.4 T magnetic field. Worthy of consideration is the fact that in the study of Neuner and co-workers no fMRI acquisition sequence was applied, that means that the EEG data were free of gradient artefacts. Future studies will need to repeat measurements during a running EPI sequence to evaluate gradient artefacts for removal. Since the gradient hardware – gradient insert and amplifiers – in the 9.4 T system is identical to those in a 3 T Tim Trio system, no significant change in the gradient artefacts is expected. This standard set-up achieves a maximum gradient strength of 40 mT/m at a slew rate of 200 mT/m/ms. However, the desire of higher slew rates in order to achieve shorter echo times has led to the development of significantly stronger gradient systems. One example is an insert head gradient system (Kimmlingen et al., 2002) which achieves a maximum field gradient of 90 mT/m and a slew rate of 800 mT/m/ms. Since the voltage of the signal induced in the EEG leads is proportional to the rate of change of the magnetic field, these research gradient systems are capable of increasing the magnitude of artefacts by a factor of four.

In a follow-up study conducted by Arrubla and co-workers, focusing on visual evoked potentials (VEPs) (Fig. 5) and the P300 in an auditory oddball paradigm (Fig. 7), it was established that also the speed of primary visual perception and early cognitive processing is not altered by the 9.4 T static magnetic field (Arrubla et al., 2013). The topographies of the ERPs varied to quite a degree between both field strengths, which was due to the remaining artefacts in the 9.4 T signals; it opens up the field for further research into optimizing the processing of raw signals recorded at ultra-high magnetic fields. Recent research in the field of cognitive functions has shown that ultra-high fields do not seem to have any persisting influence on the attention networks of human cognition immediately after exposure (Schlamann et al., 2010). Nevertheless the focus of such investigations was the performance of neuro-cognitive testing before and after the MRI examinations, not during direct exposure to the magnetic field. This is an important prerequisite for future fMRI studies at ultra-high fields and has been one task to be investigated at the prototype 9.4 T MR–PET system in Jülich, Germany. This task was initiated by the ethics committee and administrative body (BfARM, Germany) in order to approve the use of the pilot system. Heinrich and co-workers conducted a study in which the subjects performed a series of tests at magnetic fields from 0 to 7 T (Heinrich et al., 2013). These tests covered cognitive functions such as memory, eye–hand coordination, attention, reaction time, and visual discrimination. They found that static magnetic fields do not have a significant effect on cognitive function at any field strength. The results of Arrubla and co-workers are in line with these finding since the P300 is believed to be a neural signature of attention and working memory required for an appropriate response to environment stimuli (Polich, 2007).

Challenges

A major challenge for recording EEG data at ultra-high field is removal of the artefacts resulting from the magnetic field. As discussed

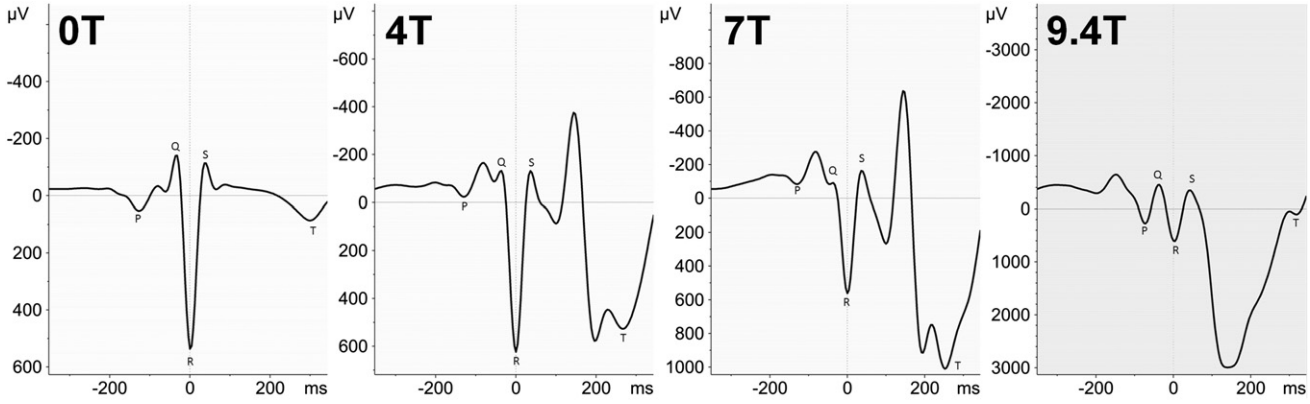

Fig. 3. Electrocardiographic signal recorded from the chest of one subject at different magnetic field strengths.

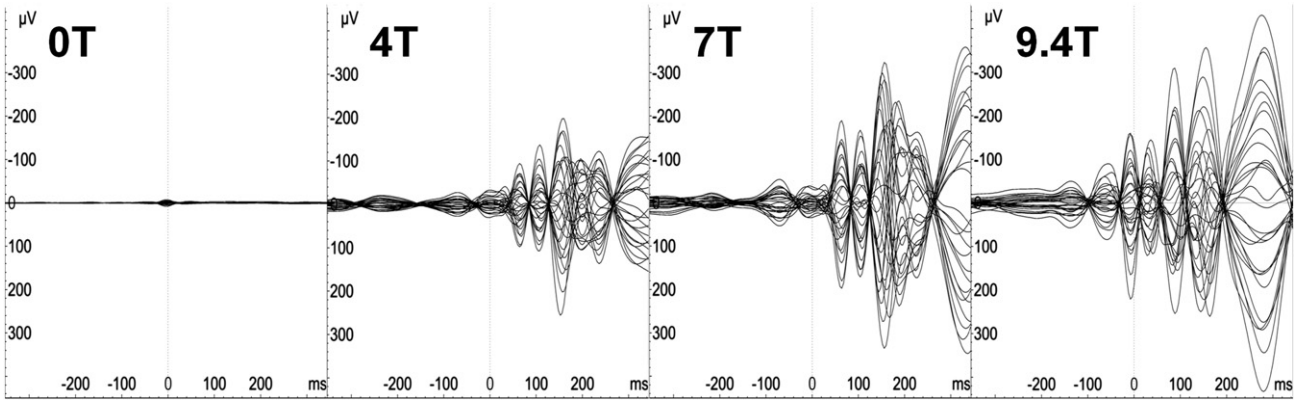

Fig. 4. Variability of the cardiac-related artefact at different static magnetic fields.

by Mullinger and co-workers, the magnitude of electromagnetic induction due to the movement of conductive material within the scanner increases with the strength of the magnetic field. That means that any movement of the subject's head or vibration of the elements of the EEG system will result in large interference (Mullinger et al., 2008b). On the other hand the standard correction methods for the cardiac-related artefact do not seem to be completely accurate for artefact removal, making the identification of real EEG events in the recordings performed at ultra-high magnetic fields difficult. Although ICA has been demonstrated to be a powerful tool for the correction of a variety of data artefacts (Iriarte et al., 2003; Jung et al., 2000), it still has the drawback of relying much on the algorithm applied for decomposition. Also because ICA assumes stationarity of the sources the applications are limited. One of the mayor weaknesses is that the selection of components that contribute to the signal of interest is made subjectively. Mixed signals might be over- or undercorrected.

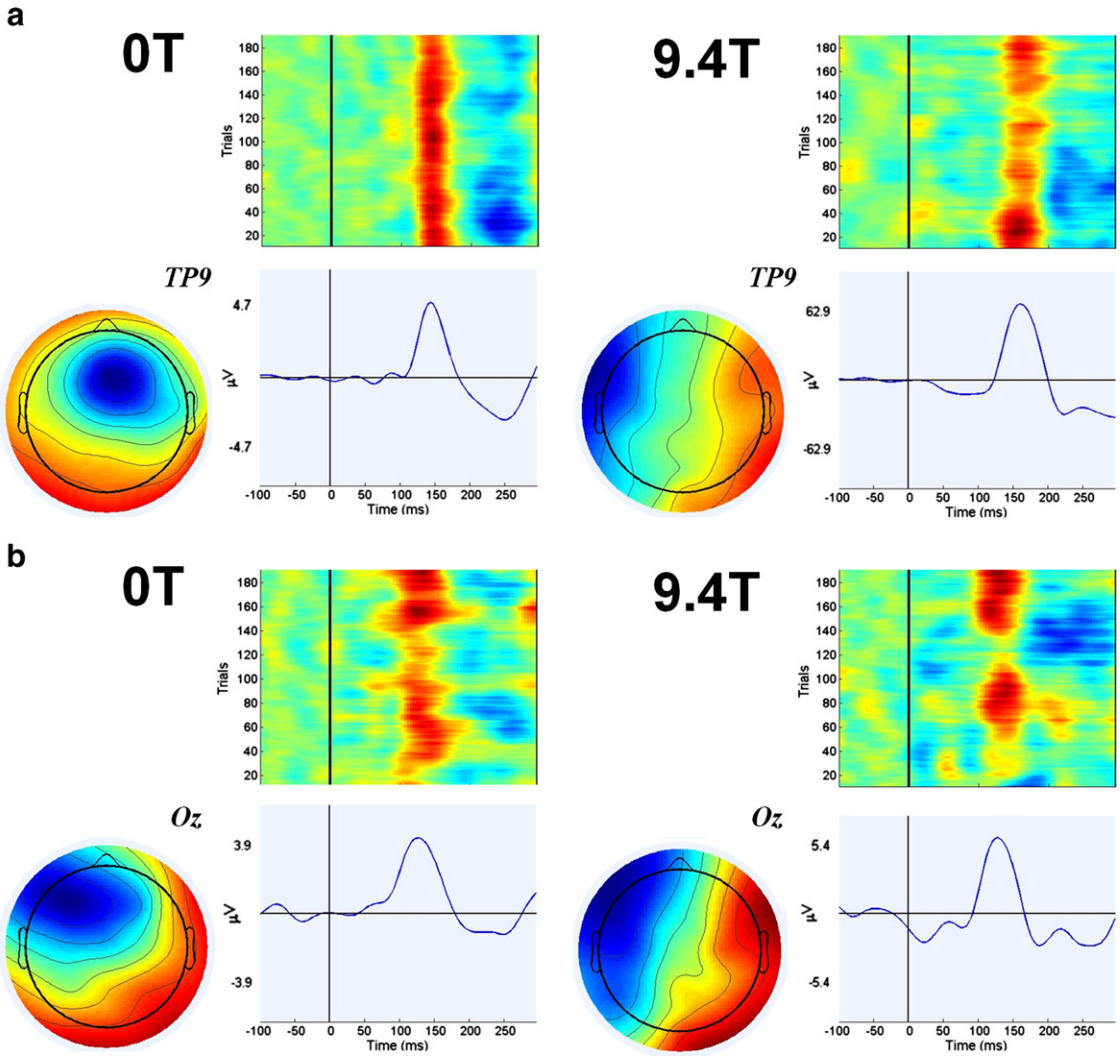

Fig. 5. Example of (a) auditory evoked potentials and (b) visual evoked potentials at 0 T and at 9.4 T recorded from one subject. The plot over the ERP signal shows the consistency of the response across the trials.

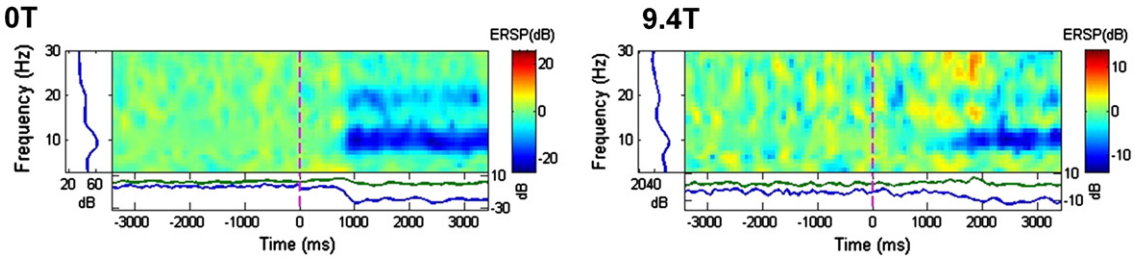

Fig. 6. Example of event related spectral perturbation (ERSP) analysis in one subject at 0 T and 9.4 T. The time–frequency analysis shows desynchronisation of the frequencies between 8 and 10 Hz (alpha) around the opening-the-eyes event. The data recorded at 9.4 T were corrected for the cardiac-related artefact using ICA.

An automated ICA-based method for artefacts deletion would be of great help for processing and analysing EEG data recorded at ultra-high magnetic fields.

Outlook — From simultaneous bimodal techniques to trimodal imaging

A new generation of hybrid imaging systems that combine complementary methods, i.e. MR and positron emission tomography (PET) are emerging. Each method itself poses an important milestone in diagnostics and research in clinical neuroscience. The hybrid system is designed for the simultaneous acquisition of MR and PET data (Herzog et al., 2010, 2011; Sauter et al., 2010; Schiepers and Dahlbom, 2011). Although MR and PET complement each other in terms of their spatial and temporal resolution, the domain of PET is the assessment at molecular level. The underlying molecular basis of fMRI paradigms or resting state is accessible through the integration of PET and MR. PET provides the possibility of investigate a number of brain aspects depending on the radiotracer used. Using 18-FDG-PET, for example, is the gold standard procedure to investigate brain metabolism. 11C-raclopride allows one to investigate striatal D2-receptors while the GABAergic system is accessible via 11C-flumazenil. Although the benefit of PET is its highly specific information on the molecular level, its spatial resolution is low and it comes with the disadvantage of radiation exposure to the volunteers/patients. Thus, research hypotheses need to be addressed efficiently when investigating healthy subjects. The new technological developments in terms of more efficient MR sequences foster this approach. Thus, a comprehensive imaging protocol covering e.g. 11C-flumazenil PET with structural MR-imaging (T1-weighted, T2-weighted), ultrashort TE (UTE) sequence for attenuation correction, diffusion tensor imaging, spectroscopy and task-related fMRI (motor paradigm) as well as resting state fMRI in a time frame of 60 min total acquisition time becomes feasible. Although the hybrid MR–PET approaches result in highly specific molecular information and excellent spatial resolution, the temporal resolution remains suboptimal. Therefore a trimodal approach consisting of MR–PET–EEG is desirable. The successful integration of an MR-compatible EEG-system in a hybrid 3 T MR–PET system has been reported (Neuner et al., 2013b). PET electronics do not disturb the electrophysiological signals and the attenuation caused by the EEG-electrodes in the PET signal is negligible.

A trimodal approach holds high value especially for the investigation of cognitive, social or emotional paradigms in which novelty plays an important role or for studies applying pharmacological challenges. One example for pharmacological studies could be the influence of nicotine and nicotine withdrawal on cognition or the effect of methylphenidate in healthy controls and individuals with attention-deficit-hyperactivity disorder on cognition and social interaction. Pharmacological interventions might lead to a change in receptor status, and would open the possibility to investigate its influence on physiological conditions (Laruelle et al., 1997). The pharmacological challenge might, for example, affect the cerebrovascular flow and modify the PET parameters as well as the BOLD characteristics. A truly simultaneous approach ensures the same physiological conditions and allows one in addition to investigate the perfusion changes via MR-derived methods such as arterial spin labelling (ASL).

Apart from research driven approaches, clinical applications would also benefit from the trimodal approach. One possibility is the presurgical diagnostic examination of pharmaco-resistant epilepsy patients (Rosenkranz and Lemieux, 2010). Combined MR–11C-flumazenil-PET–EEG approach would offer the advantage of identifying the underlying epileptogenic focus via EEG-informed fMRI analysis and would provide binding potential information via 11C-flumazenil as a potential biomarker for the epileptogenic regions (Savic et al., 1995).

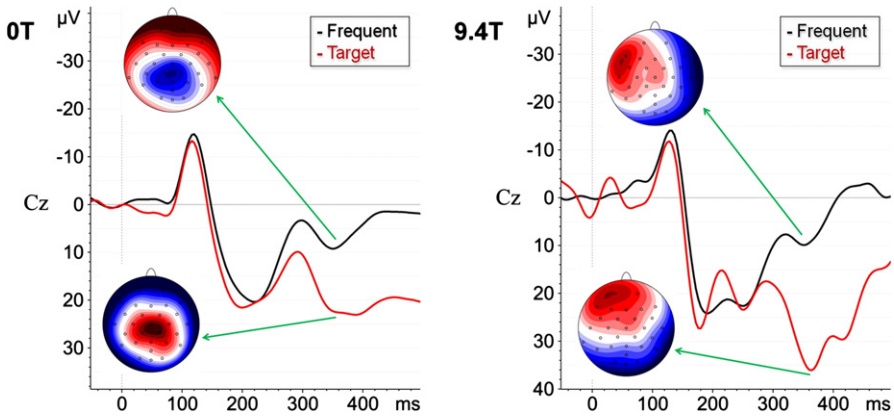

Fig. 7. Example of P300 evoked potentials recorded from one subject during an auditory oddball paradigm at 0 T and 9.4 T.

MR–PET–EEG is now becoming available at clinical field strengths such as 3 T, and for research purposes at 9.4 T (Siemens, Erlangen, Germany).

Acknowledgments

We acknowledge the Marie Curie Initial Training Network (MC-ITN) "Methods in Neuroimaging", project number MC-ITN-238593. We thank the Bundesministerium für Bildung und Forschung (BMBF), grant number 13N912. We kindly acknowledge Siemens for the 9.4 T scanner project. We thank the Deutsche Forschungsgemeinschaft, grant DFG SH 79/2-2.

Conflict of interest

None for the current study by all authors.

References

Allen, P.J., Polizzi, G., Krakow, K., Fish, D.R., Lemieux, L., 1998. Identification of EEG events in the MR scanner: the problem of pulse artifact and a method for its subtraction. NeuroImage 8, 229–239.
Allen, P.J., Josephs, O., Turner, R., 2000. A method for removing imaging artifact from continuous EEG recorded during functional MRI. NeuroImage 12, 230–239.
Arrubla, J., Neuner, I., Hahn, D., Boers, F., Shah, N.J., 2013. Recording visual evoked potentials and auditory evoked P300 at 9.4 T static magnetic field. PLoS One 8, 7.
Bagshaw, A.P., Warbrick, Tracy, 2007. Single trial variability of EEG and fMRI responses to visual stimuli. NeuroImage 38, 280–292.
Basser, P.J., Mattiello, J., LeBihan, D., 1994. MR diffusion tensor spectroscopy and imaging. Biophys. J. 66, 259–267.
Biswal, B., Yetkin, F.Z., Haughton, V.M., Hyde, J.S., 1995. Functional connectivity in the motor cortex of resting human brain using echo-planar MRI. Magn. Reson. Med. 34, 537–541.
Bonmassar, G., Purdon, P.L., Jääskeläinen, I.P., Chiappa, K., Solo, V., Brown, E.N., Belliveau, J.W., 2002. Motion and ballistocardiogram artifact removal for interleaved recording of EEG and EPs during MRI. NeuroImage 16, 1127–1141.
Braakman, H.M.H., Van der Kruijs, S.J.M., Vaessen, M.J., Jansen, J.F.A., Debeij-van Hall, M.H.J.A., Vles, J.S.H., Aldenkamp, A.P., Backes, W.H., Hofman, P.A.M., 2012. Microstructural and functional MRI studies of cognitive impairment in epilepsy. Epilepsia 53, 1690–1699.
Brookes, M.J., Mullinger, K.J., Stevenson, C.M., Morris, P.G., Bowtell, R., 2008. Simultaneous EEG source localisation and artifact rejection during concurrent fMRI by means of spatial filtering. NeuroImage 40, 1090–1104.
Brookes, M.J., Vrba, J., Mullinger, K.J., Geirsdóttir, G.B., Yan, W.X., Stevenson, C.M., Bowtell, R., Morris, P.G., 2009. Source localisation in concurrent EEG/fMRI: applications at 7 T. NeuroImage 45, 440–452.
Buzsáki, G., Draguhn, A., 2004. Neuronal oscillations in cortical networks. Science 304, 1926–1929.
Caballero-Gaudes, C., Van de Ville, D., Grouiller, F., Thornton, R., Lemieux, L., Seeck, M., Lazeyras, F., Vulliemoz, Serge, 2013. Mapping interictal epileptic discharges using mutual information between concurrent EEG and fMRI. NeuroImage 68, 248–262.
Cabeza, R., Nyberg, L., 2000. Neural bases of learning and memory: functional neuroimaging evidence. Curr. Opin. Neurol. 13, 415–421.
Carmichael, D.W., Vulliemoz, S., Rodionov, R., Thornton, J.S., McEvoy, A.W., Lemieux, L., 2012. Simultaneous intracranial EEG–fMRI in humans: protocol considerations and data quality. NeuroImage 63, 301–309.
Chaudhary, U.J., Rodionov, R., Carmichael, D.W., Thornton, R.C., Duncan, J.S., Lemieux, L., 2012. Improving the sensitivity of EEG–fMRI studies of epileptic activity by modelling eye blinks, swallowing and other video-EEG detected physiological confounds. NeuroImage 61, 1383–1393.
Cochrane, C.J., Ebmeier, K.P., 2013. Diffusion tensor imaging in parkinsonian syndromes: a systematic review and meta-analysis. Neurology 80, 857–864.
Debener, S., Herrmann, C.S., 2008. Integration of EEG and fMRI. Editorial. Int. J. Psychophysiol. 67, 159–160.
Debener, S., Ullsperger, M., Siegel, M., Engel, A.K., 2006. Single-trial EEG–fMRI reveals the dynamics of cognitive function. Trends Cogn. Sci. 10, 558–563.
Debener, S., Ullsperger, M., Siegel, M., Engel, A.K., 2007. Towards single-trial analysis in cognitive brain research. Trends Cogn. Sci. 11, 502–503.
Debener, S., Mullinger, K.J., Niazy, Rami K., Bowtell, R.W., 2008. Properties of the ballistocardiogram artefact as revealed by EEG recordings at 1.5, 3 and 7 T static magnetic field strength. Int. J. Psychophysiol. 67, 189–199.
Eichele, T., Calhoun, V.D., Debener, S., 2009. Mining EEG–fMRI using independent component analysis. Int. J. Psychophysiol. 73, 53–61.
Harel, N., Uğurbil, K., Uludağ, K., Yacoub, E., 2006. Frontiers of brain mapping using MRI. J. Magn. Reson. Imaging 23, 945–957.
Heinrich, A., Szostek, A., Meyer, P., Nees, F., Rauschenberg, J., Gröbner, J., Gilles, M., Paslakis, G., Deuschle, M., Semmler, W., Flor, H., 2013. Cognition and sensation in very high static magnetic fields: a randomized case–crossover study with different field strengths. Radiology 266, 236–245.
Herzog, H., Pietrzyk, U., Shah, N.J., Ziemons, K., 2010. The current state, challenges and perspectives of MR–PET. NeuroImage 49, 2072–2082.
Herzog, H., Langen, K.J., Weirich, C., Rota Kops, E., Kaffanke, J., Tellmann, L., Scheins, J., Neuner, I., Stoffels, G., Fischer, K., Caldeira, L., Coenen, H.H., Shah, N.J., 2011. High resolution BrainPET combined with simultaneous MRI. Nuklearmedizin 50, 74–82.
Huang-Hellinger, F.R., Breiter, H.C., McCormack, G., Cohen, M.S., Kwong, K.K., Sutton, J.P., Savoy, R.L., Weisskoff, R.M., Davis, T.L., Baker, J.R., Belliveau, J.W., Rosen, B.R., 1995. Simultaneous functional magnetic resonance imaging and electrophysiological recording. Hum. Brain Mapp. 3, 13–23.
Huettel, S.A., 2012. Event-related fMRI in cognition. NeuroImage 62, 1152–1156.
Huster, R.J., Debener, S., Eichele, T., Herrmann, C.S., 2012. Methods for simultaneous EEG–fMRI: an introductory review. J. Neurosci. 32, 6053–6060.
Iriarte, J., Urrestarazu, E., Valencia, M., Alegre, M., Malanda, A., Viteri, C., Artieda, J., 2003. Independent component analysis as a tool to eliminate artifacts in EEG: a quantitative study. J. Clin. Neurophysiol. 20, 249–257.
Ives, J.R., Warach, S., Schmitt, F., Edelman, R.R., Schomer, D.L., 1993. Monitoring the patient's EEG during echo planar MRI. Electroencephalogr. Clin. Neurophysiol. 87, 417–420.
Juckel, G., Karch, S., Kawohl, W., Kirsch, V., Jäger, L., Leicht, G., Lutz, J., Stammel, A., Pogarell, O., Ertl, M., Reiser, M., Hegerl, U., Möller, H.J., Mulert, C., 2012. Age effects on the P300 potential and the corresponding fMRI BOLD-signal. NeuroImage 60, 2027–2034.
Jung, T.P., Makeig, S., Humphries, C., Lee, T.W., McKeown, M.J., Iragui, V., Sejnowski, T.J., 2000. Removing electroencephalographic artifacts by blind source separation. Psychophysiology 37, 163–178.
Kilimann, I., Likitjaroen, Y., Hampel, H., Teipel, S., 2013. Diffusion tensor imaging to determine effects of antidementive treatment on cerebral structural connectivity in Alzheimer's disease. Curr. Pharm. Des. (in press).
Kimmlingen, R., Gebhardt, M., Schuster, J., Brand, M., Schmitt, F., Haase, A., 2002. Gradient system providing continuously variable field characteristics. Magn. Reson. Med. 47, 800–808.
Koike, T., Kan, S., Misaki, M., Miyauchi, S., 2011. Connectivity pattern changes in default-mode network with deep non-REM and REM sleep. Neurosci. Res. 69, 322–330.
Kuswanto, C.N., Teh, I., Lee, T.-S., Sim, K., 2012. Diffusion tensor imaging findings of white matter changes in first episode schizophrenia: a systematic review. Clin. Psychopharmacol. Neurosci. 10, 13–24.
Laruelle, M., Iyer, R.N., al-Tikriti, M.S., Zea-Ponce, Y., Malison, R., Zoghbi, S.S., Baldwin, R.M., Kung, H.F., Charney, D.S., Hoffer, P.B., Innis, R.B., Bradberry, C.W., 1997. Microdialysis and SPECT measurements of amphetamine-induced dopamine release in nonhuman primates. Synapse 25, 1–14.
Laufs, H., 2012. A personalized history of EEG–fMRI integration. NeuroImage 62, 1056–1067.
Laufs, H., Daunizeau, J., Carmichael, D.W., Kleinschmidt, A., 2008. Recent advances in recording electrophysiological data simultaneously with magnetic resonance imaging. NeuroImage 40, 515–528.
Leclercq, Y., Balteau, E., Dang-Vu, T., Schabus, M., Luxen, A., Maquet, P., Phillips, C., 2009. Rejection of pulse related artefact (PRA) from continuous electroencephalographic (EEG) time series recorded during functional magnetic resonance imaging (fMRI) using constraint independent component analysis (cICA). NeuroImage 44, 679–691.
Lemieux, L., Allen, P.J., Franconi, F., Symms, M.R., Fish, D.R., 1997. Recording of EEG during fMRI experiments: patient safety. Magn. Reson. Med. 38, 943–952.
Levan, P., Maclaren, J., Herbst, M., Sostheim, R., Zaitsev, M., Hennig, J., 2013. Ballistocardiographic artifact removal from simultaneous EEG–fMRI using an optical motion-tracking system. NeuroImage 75, 1–11.
Luo, Q., Glover, G.H., 2012. Influence of dense-array EEG cap on fMRI signal. Magn. Reson. Med. 68, 807–815.
Makeig, S., Debener, S., Onton, J., Delorme, A., 2004. Mining event-related brain dynamics. Trends Cogn. Sci. 8, 204–210.
Meltzer, J.A., Fonzo, G.A., Constable, R.T., 2009. Transverse patterning dissociates human EEG theta power and hippocampal BOLD activation. Psychophysiology 46, 153–162.
Michel, C.M., Murray, M.M., 2012. Towards the utilization of EEG as a brain imaging tool. NeuroImage 61, 371–385.
Moosmann, M., Schönfelder, V.H., Specht, K., Scheeringa, R., Nordby, H., Hugdahl, K., 2009. Realignment parameter-informed artefact correction for simultaneous EEG–fMRI recordings. NeuroImage 45, 1144–1150.
Mullinger, K., Brookes, M., Stevenson, C., Morgan, P., Bowtell, R., 2008a. Exploring the feasibility of simultaneous electroencephalography/functional magnetic resonance imaging at 7 T. Magn. Reson. Imaging 26, 968–977.
Mullinger, K., Debener, S., Coxon, R., Bowtell, R., 2008b. Effects of simultaneous EEG recording on MRI data quality at 1.5, 3 and 7 Tesla. Int. J. Psychophysiol. 67, 178–188.
Mullinger, K.J., Havenhand, J., Bowtell, R., 2013. Identifying the sources of the pulse artefact in EEG recordings made inside an MR scanner. NeuroImage 71, 75–83.
Müri, R.M., Felblinger, J., Rösler, K.M., Jung, B., Hess, C.W., Boesch, C., 1998. Recording of electrical brain activity in a magnetic resonance environment: distorting effects of the static magnetic field. Magn. Reson. Med. 39, 18–22.
Musall, S., Von Pföstl, V., Rauch, A., Logothetis, N.K., Whittingstall, K., 2013. Effects of neural synchrony on surface EEG. Cereb. Cortex (in press).
Neuner, I., Stöcker, T., Kellermann, T., Kircher, T., Zilles, Karl, Schneider, F., Shah, N.J., 2007. Wechsler Memory Scale Revised Edition: neural correlates of the visual paired associates subtest adapted for fMRI. Brain Res. 1177, 66–78.
Neuner, I., Kupriyanova, Y., Stöcker, T., Huang, Ruiwang, Posnansky, O., Schneider, F., Tittgemeyer, M., Shah, N.J., 2010a. White-matter abnormalities in Tourette syndrome extend beyond motor pathways. NeuroImage 51, 1184–1193.
Neuner, I., Stöcker, T., Kellermann, T., Ermer, V., Wegener, H.P., Eickhoff, S.B., Schneider, F., Shah, N.J., 2010b. Electrophysiology meets fMRI: neural correlates of the startle reflex assessed by simultaneous EMG–fMRI data acquisition. Hum. Brain Mapp. 31, 1675–1685.

Neuner, I., Warbrick, T., Arrubla, J., Felder, J., Celik, A., Reske, M., Boers, F., Shah, N.J., 2013a. EEG acquisition in ultra-high static magnetic fields up to 9.4 T. NeuroImage 68, 214–220.
Neuner, I., Warbrick, T., Tellmann, L., Rota Kops, E., Arrubla, J., Boers, F., Herzog, H., Shah, N.J., 2013b. Multimodal imaging: simultaneous EEG in a 3 T hybrid MR–PET system. Nucl. Inst. Methods Phys. Res. A 702, 37–38.
Niazy, R.K., Beckmann, C.F., Iannetti, G.D., Brady, J.M., Smith, S.M., 2005. Removal of FMRI environment artifacts from EEG data using optimal basis sets. NeuroImage 28, 720–737.
Nierhaus, T., Gundlach, C., Goltz, D., Thiel, S.D., Pleger, B., Villringer, Arno, 2013. Internal ventilation system of MR scanners induces specific EEG artifact during simultaneous EEG–fMRI. NeuroImage 74, 70–76.
Nöth, U., Laufs, H., Stoermer, R., Deichmann, R., 2012. Simultaneous electroencephalography-functional MRI at 3 T: an analysis of safety risks imposed by performing anatomical reference scans with the EEG equipment in place. J. Magn. Reson. Imaging 35, 561–571.
Nunez, P.L., Silberstein, R.B., 2000. On the relationship of synaptic activity to macroscopic measurements: does co-registration of EEG with fMRI make sense? Brain Topogr. 13, 79–96.
Ochsner, K.N., Silvers, J.A., Buhle, J.T., 2012. Functional imaging studies of emotion regulation: a synthetic review and evolving model of the cognitive control of emotion. Ann. N. Y. Acad. Sci. 1251, E1–E24.
Ogawa, S., Menon, R.S., Tank, D.W., Kim, S.G., Merkle, H., Ellermann, J.M., Ugurbil, K., 1993. Functional brain mapping by blood oxygenation level-dependent contrast magnetic resonance imaging. A comparison of signal characteristics with a biophysical model. Biophys. J. 64, 803–812.
Olman, C.A., Harel, N., Feinberg, D.A., He, S., Zhang, P., Ugurbil, Kamil, Yacoub, E., 2012. Layer-specific fMRI reflects different neuronal computations at different depths in human V1. PLoS One 7, e32536.
Peters, J.C., Reithler, J., Schuhmann, T., De Graaf, T., Uludag, K., Goebel, R., Sack, A.T., 2013. On the feasibility of concurrent human TMS-EEG–fMRI measurements. J. Neurophysiol. 109, 1214–1227.
Polich, J., 2007. Updating P300: an integrative theory of P3a and P3b. Clin. Neurophysiol. 118, 2128–2148.
Raichle, M.E., MacLeod, A.M., Snyder, A.Z., Powers, W.J., Gusnard, D.A., Shulman, G.L., 2001. A default mode of brain function. Proc. Natl. Acad. Sci. U. S. A. 98, 676–682.
Ritter, P., Becker, R., Freyer, F., Villringer, A., 2010. EEG quality: the image acquisition artefact. In: Mulert, C., Lemieux, L. (Eds.), EEG–fMRI. Springer, Berlin, pp. 153–171.
Rosenkranz, K., Lemieux, L., 2010. Present and future of simultaneous EEG–fMRI. MAGMA 23, 309–316.
Rushworth, M.F., Mars, R.B., Sallet, J., 2013. Are there specialized circuits for social cognition and are they unique to humans? Curr. Opin. Neurobiol. 23, 436–442.
Sadaghiani, S., Hesselmann, G., Friston, K.J., Kleinschmidt, Andreas, 2010a. The relation of ongoing brain activity, evoked neural responses, and cognition. Front. Syst. Neurosci. 4, 20.
Sadaghiani, S., Scheeringa, R., Lehongre, K., Morillon, B., Giraud, A.L., Kleinschmidt, Andreas, 2010b. Intrinsic connectivity networks, alpha oscillations, and tonic alertness: a simultaneous electroencephalography/functional magnetic resonance imaging study. J. Neurosci. 30, 10243–10250.
Sauter, A.W., Wehrl, H.F., Kolb, A., Judenhofer, M.S., Pichler, B.J., 2010. Combined PET/MRI: one step further in multimodality imaging. Trends Mol. Med. 16, 508–515.
Savic, I., Thorell, J.O., Roland, P., 1995. [11C]flumazenil positron emission tomography visualizes frontal epileptogenic regions. Epilepsia 36, 1225–1232.
Schiepers, C., Dahlbom, M., 2011. Molecular imaging in oncology: the acceptance of PET/CT and the emergence of MR/PET imaging. Eur. Radiol. 21, 548–554.
Schlamann, M., Voigt, M.A., Maderwald, S., Bitz, A.K., Kraff, O., Ladd, S.C., Ladd, M.E., Forsting, M., Wilhelm, H., 2010. Exposure to high-field MRI does not affect cognitive function. J. Magn. Reson. Imaging 31, 1061–1066.
Selvaraj, S., Arnone, D., Job, D., Stanfield, A., Farrow, T.F., Nugent, A.C., Scherk, H., Gruber, O., Chen, X., Sachdev, P.S., Dickstein, D.P., Malhi, G.S., Ha, T.H., Ha, K., Phillips, M.L., McIntosh, A.M., 2012. Grey matter differences in bipolar disorder: a meta-analysis of voxel-based morphometry studies. Bipolar Disord. 14, 135–145.
Shah, N.J., Marshall, J.C., Zafiris, O., Schwab, A., Zilles, K., Markowitsch, H.J., Fink, G.R., 2001. The neural correlates of person familiarity. A functional magnetic resonance imaging study with clinical implications. Brain 124, 804–815.
Singh, K.D., 2012. Which "neural activity" do you mean? fMRI, MEG, oscillations and neurotransmitters. NeuroImage 62, 1121–1130.
Tagliazucchi, E., Von Wegner, F., Morzelewski, A., Borisov, S., Jahnke, K., Laufs, H., 2012. Automatic sleep staging using fMRI functional connectivity data. NeuroImage 63, 63–72.
Tenforde, T.S., Gaffey, C.T., Moyer, B.R., Budinger, T.F., 1983. Cardiovascular alterations in Macaca monkeys exposed to stationary magnetic fields: experimental observations and theoretical analysis. Bioelectromagnetics 4, 1–9.
Thornton, R., Laufs, H., Rodionov, R., Cannadathu, S., Carmichael, D.W., Vulliemoz, S., Salek-Haddadi, A., McEvoy, A.W., Smith, S.M., Lhatoo, S., Elwes, R.D.C., Guye, M., Walker, M.C., Lemieux, L., Duncan, J.S., 2010a. EEG correlated functional MRI and postoperative outcome in focal epilepsy. J. Neurol. Neurosurg. Psychiatry 81, 922–927.
Thornton, R., Rodionov, R., Laufs, H., Vulliemoz, S., Vaudano, A., Carmichael, D., Cannadathu, S., Guye, M., McEvoy, A., Lhatoo, S., Bartolomei, F., Chauvel, P., Diehl, B., De Martino, F., Elwes, R.D.C., Walker, M.C., Duncan, J.S., Lemieux, L., 2010b. Imaging haemodynamic changes related to seizures: comparison of EEG-based general linear model, independent component analysis of fMRI and intracranial EEG. NeuroImage 53, 196–205.
Van Audekerkea, J., Peeters, R., Verhoye, M., Sijbers, J., Van der Linden, A., 2000. Special designed RF-antenna with integrated non-invasive carbon electrodes for simultaneous magnetic resonance imaging and electroencephalography acquisition at 7 T. Magn. Reson. Imaging 18, 887–891.
Vasios, C.E., Angelone, L.M., Purdon, P.L., Ahveninen, J., Belliveau, J.W., Bonmassar, G., 2006. EEG/(f)MRI measurements at 7 Tesla using a new EEG cap ("InkCap"). NeuroImage 33, 1082–1092.
Vulliemoz, S., Carmichael, D.W., Rosenkranz, K., Diehl, B., Rodionov, R., Walker, M.C., McEvoy, A.W., Lemieux, L., 2011. Simultaneous intracranial EEG and fMRI of interictal epileptic discharges in humans. NeuroImage 54, 182–190.
Yacoub, E., Van De Moortele, P.F., Shmuel, A., Uğurbil, K., 2005. Signal and noise characteristics of Hahn SE and GE BOLD fMRI at 7 T in humans. NeuroImage 24, 738–750.
Yan, W.X., Mullinger, K.J., Geirsdottir, G.B., Bowtell, R., 2010. Physical modeling of pulse artefact sources in simultaneous EEG/fMRI. Hum. Brain Mapp. 31, 604–620.
Yang, J., Pan, P., Song, W., Huang, Rui, Li, J., Chen, K., Gong, Q., Zhong, J., Shi, H., Shang, H., 2012. Voxelwise meta-analysis of gray matter anomalies in Alzheimer's disease and mild cognitive impairment using anatomic likelihood estimation. J. Neurol. Sci. 316, 21–29.
Yeşilyurt, B., Whittingstall, K., Uğurbil, K., Logothetis, N.K., Uludağ, K., 2010. Relationship of the BOLD signal with VEP for ultrashort duration visual stimuli (0.1 to 5 ms) in humans. J. Cereb. Blood Flow Metab. 30, 449–458.